

Article

Power System Voltage Stability Margin Estimation Using Adaptive Neuro-Fuzzy Inference System Enhanced with Particle Swarm Optimization

Oludamilare Bode Adewuyi ^{1,*}, Komla A. Folly ¹, David T. O. Oyedokun ¹
and Emmanuel Idowu Ogunwole ²

¹ Department of Electrical Engineering, University of Cape Town, Cape Town 7701, South Africa

² Department of Electrical, Electronic and Computer Engineering, Cape Peninsula University of Technology, Bellville Campus, Cape Town 7535, South Africa

* Correspondence: adewuyiobode@gmail.com

Abstract: In the current era of e-mobility and for the planning of sustainable grid infrastructures, developing new efficient tools for real-time grid performance monitoring is essential. Thus, this paper presents the prediction of the voltage stability margin (VSM) of power systems by the critical boundary index (CBI) approach using the machine learning technique. Prediction models are based on an adaptive neuro-fuzzy inference system (ANFIS) and its enhanced model with particle swarm optimization (PSO). Standalone ANFIS and PSO-ANFIS models are implemented using the fuzzy ‘c-means’ clustering method (FCM) to predict the expected values of CBI as a veritable tool for measuring the VSM of power systems under different loading conditions. Six vital power system parameters, including the transmission line and bus parameters, the power injection, and the system voltage derived from load flow analysis, are used as the ANFIS model implementation input. The performances of the two ANFIS models on the standard IEEE 30-bus and the Nigerian 28-bus systems are evaluated using error and regression analysis metrics. The performance metrics are the root mean square error (*RMSE*), mean absolute percentage error (*MAPE*), and Pearson correlation coefficient (*R*) analyses. For the IEEE 30-bus system, *RMSE* is estimated to be 0.5833 for standalone ANFIS and 0.1795 for PSO-ANFIS; *MAPE* is estimated to be 13.6002% for ANFIS and 5.5876% for PSO-ANFIS; and *R* is estimated to be 0.9518 and 0.9829 for ANFIS and PSO-ANFIS, respectively. For the NIGERIAN 28-bus system, the *RMSE* values for ANFIS and PSO-ANFIS are 5.5024 and 2.3247, respectively; *MAPE* is 19.9504% and 8.1705% for both ANFIS and PSO-ANFIS variants, respectively, and the *R* is estimated to be 0.9277 for ANFIS and 0.9519 for ANFIS-PSO, respectively. Thus, the PSO-ANFIS model shows a superior performance for both test cases, as indicated by the percentage reduction in prediction error, although at the cost of a higher simulation time.

Keywords: power system stability; voltage stability margin; critical boundary index; adaptive neuro-fuzzy inference system; fuzzy clustering; particle swarm optimization



Citation: Adewuyi, O.B.; Folly, K.A.; Oyedokun, D.T.O.; Ogunwole, E.I. Power System Voltage Stability Margin Estimation Using Adaptive Neuro-Fuzzy Inference System Enhanced with Particle Swarm Optimization. *Sustainability* **2022**, *14*, 15448. <https://doi.org/10.3390/su142215448>

Academic Editor: Nicu Bizon

Received: 3 October 2022

Accepted: 18 November 2022

Published: 21 November 2022

Publisher’s Note: MDPI stays neutral with regard to jurisdictional claims in published maps and institutional affiliations.



Copyright: © 2022 by the authors. Licensee MDPI, Basel, Switzerland. This article is an open access article distributed under the terms and conditions of the Creative Commons Attribution (CC BY) license (<https://creativecommons.org/licenses/by/4.0/>).

1. Introduction

Challenges of voltage instability are majorly responsible for blackouts and techno-economic depletions in the power systems of many nations [1]. Thus, a vital yardstick for evaluating the viability of a power system network (grid infrastructures) is the amount of available voltage stability margin (VSM). VSM is often considered to measure how long a particular power system can operate before suffering voltage instability in the face of continuously changing load demand, and generation dynamics [2,3]. Theoretically, it can be estimated as the distance between a current operating point and the nearest point of voltage collapse as the real and reactive loading is continuously increased [4]. Generally, the capacity of existing grid infrastructures to accommodate increased load and sometimes increased generation, especially from renewable energy sources, is very limited.

However, with the load flow analysis, the VSM of a grid can be sufficiently monitored towards setting up appropriate control for secure operation. Remarkably, significant efforts were devoted to power system security analysis over the years [5,6]. However, most approaches for investigating voltage instabilities in power systems are based on static analysis using the power transfer concept and load flow calculations. Consequently, several voltage stability indices (VSIs) were available in works of literature as products of rigorous research activities for monitoring power system security [7,8]. However, most of these tools, i.e., VSIs, have limited performance capacity for accuracy and precision regarding real networks and large/complex power systems. This underperformance of conventional VSIs is attributed to the fact that these tools are derived approximately considering few power system parameters [4]. Moreover, a vital consideration for the real-time implementation of the conventional VSI procedures, which is the computation time, is considerably large, especially for complex networks [9]. Thus, it is necessary to research the development of better performing intelligent-based techniques for effectively managing voltage stability issues in power systems.

Due to the advent of artificial intelligence (AI), intelligent predictions of future events are taking the prominent stage for critical infrastructure planning and operations in recent time [10]. Different AI-based mechanisms were successfully implemented in various areas of intelligent infrastructure management, such as transportation, water supply, food processing, chemical processing, building design and construction, etc. Common AI-based prediction models include artificial intelligence-based algorithms such as regression analysis, artificial neural networks (ANNs), support vector machines, K-means, Bayesian methods, fuzzy logic, expert systems, etc., [11]. Power system networks are expensive, complex to operate, and significantly critical public infrastructures, and voltage stability monitoring is a significant aspect of its reliable operation and protection [12]. Several predictive analytics tools have been applied in the literature for solving critical power systems problems, such as load flow analysis, contingency planning, transmission congestion management, grid reinforcement planning, etc. [13–15]. Thus, one of the imminent prospects for the effective operation of grid infrastructures is the intelligent monitoring of the voltage stability condition of the power systems under a continuously changing loading condition. Thus, in this study, the intelligent monitoring of VSM for the effective control of voltage stability conditions is viewed as an essential tool for real-life and complex power system infrastructure management. Thus, hybridized ANFIS-based intelligent predictive models are implemented for measuring the VSM of power systems based on the concept of a critical boundary index (CBI). Credible information on vital power system parameters for ANFIS training and validation is determined from the line and bus parameters and the load flow analysis solution. The developed ANFIS and PSO-ANFIS models for VSM prediction are tested on the standard IEEE 30-bus and the Nigerian 28-bus networks. Their relative performances are evaluated and compared using adequate statistical analysis.

This work aimed to establish the idea of the critical boundary index (CBI) as a veritable tool for the direct estimation of VSM and using machine learning techniques (ANFIS and its hybrid with PSO) to verify CBI's capacity for different loading conditions. Specifically, this work adopted ANFIS and its hybridization with PSO to monitor the power systems' adequate voltage stability margin under different loading conditions. Generally, the first step to voltage collapse mitigation is to achieve efficient estimations of the power system's closeness to the voltage stability limit; and this can be achieved using veritable machine learning approaches. However, the main challenge in implementing machine learning algorithms is the optimal tuning of the training parameters; thus, the PSO algorithm is combined with the ANFIS in this study to improve the training performance of the predictive analysis. The remaining contents of this paper are structured as follows: Section 2 gives an overview of the application of AI and machine learning to voltage stability analysis; Section 3 discusses the conceptualization of the mathematical models and methods adopted for this study. The simulation results are presented and discussed in Section 4, and the conclusion is presented in Section 5.

2. Artificial Intelligence/Machine Learning Approaches to Voltage Stability Analysis

Voltage stability problems are highly dynamic; however, the evaluation of voltage stability conditions of power systems can be approximated using steady-state analysis with different voltage stability indices (VSIs). Some of the notable VSIs are as; P–V and Q–V curves, line stability index (Lmn), fast voltage stability index (FVSI), voltage collapse prediction index (VCPI), novel line stability index (NLSI), line stability factor (LQP), L-index, etc., [7]. However, steady-state VSIs are approximated and relatively time-consuming; thus, they are often unreliable for the accurate and precise determination of the voltage stability condition of power systems [4]. One of the prominent attributes of AI models is the ability to work through data and establish a precise pattern for producing reliable output information within the shortest possible time. Thus, a number of research studies have applied AI vis-à-vis machine learning and deep learning techniques for voltage stability analysis, and for the efficient implementation of AI-based voltage stability analysis, the structure of the input data matters significantly. Some existing works on machine learning applications to voltage stability analysis are discussed below.

2.1. Artificial Neural Network (ANN) for Voltage Stability Margin Estimation

In reference [16], a multilayer feedforward ANN model for VSM estimation was developed using the error backpropagation learning algorithm. The power system loading conditions and the corresponding voltage stability margin were correlated using sensitivity for performance analysis. ANN models are deployed for verifying the voltage stability condition with different VSIs using the pre-estimated results from Newton Rapson load flow analysis for training an ANN model in [17,18]. In [19], a three-layer feedforward neural network was trained with calculated VSI values for detecting applicable VSM limits for power systems susceptible to voltage collapse. Online ANN models in real-time are developed for voltage stability margin estimation, adopting the data augmentation method and supervised learning based on node voltage magnitudes, and the phase angle information was presented [20–23]. For effective implementation, especially for complex multi-area power networks, handling the training data is very significant. Thus, the authors in [24] proposed an ANN model for VSI estimation that was implemented based on network data reduction and exploring the adaptive training capabilities of ANNs. The authors in [25] discussed the real-time voltage stability monitoring technique that considers the VSM as the nearest power system loading distance before the occurrence of voltage collapse. Short-term voltage stability assessment using the machine learning and deep learning techniques requires a sufficient amount of the dataset. The authors in [26] adopted a novel data technique referred to as the conditional least squares generative adversarial network (LSGAN)-based data augmentation to artificially generate a sufficient amount of required data set for the implementation of the predictive analytic model. The approach was found to be efficient for proliferating the representative and diversified training datasets while preserving the data label.

Due to the complexities of the considered procedure, which involves a continuously loading condition, researchers often deploy the orthogonalization process based on sensitivity analysis for the input data set to achieve adequate feature reduction. Another notable adaptation of AI vis-à-vis ANN and other hybridization of ML and deep learning techniques for voltage stability analysis are reported in the following literature: PSO-based recurrent neural network (PSO-RNN) [27], Salp swarm algorithm-tuned ANN (SSA-ANN) [28], ANN and Ward-type equivalent approach [29], self-organizing Kohonen-neural network (SKNN) [30], parallel self-organizing hierarchical neural network with static VAR compensator (SHNN-SVC) [31], self-organizing feature map with radial basis function (SOFM-RBF) [32], extreme learning machine (ELM) [33,34], hybrid kernel extreme learning machine approach [35], deep recurrent neural network [36], genetic algorithm-based support vector machine (GA-SVM) [37], weighted least square support vector machine (WLS-SVM) [38,39], particle swarm optimization-based support vector machine (PSO-SVM) [40], dragonfly optimization algorithm and support vector regression (DFO-SVR) [41], random

forest algorithms [42–45], deep learning, and convolution neural networks [26,46,47] and more. The authors in [48] developed a deep learning model for short-term voltage stability (STVS) assessment in real-time using a long short-term memory (LSTM) model based on the understanding of the latent temporal dependencies of power systems' behavior on the post-disturbance system dynamics. The authors deployed a semi-supervised cluster algorithm for label classification for different STVS instances in order to obtain relevant quantitative criteria.

2.2. Fuzzy Expert System and ANFIS for Voltage Stability Margin Estimation

One of the robust ML techniques rapidly gaining research attention in recent times is the fuzzy inference system (FIS). The FIS involves adopting the concept of fuzzy logic and ANN for the nonlinear mapping of a given set of input information to meet the appropriate output data [49]. A prominent member of the fuzzy expert systems family that was found to be easily adaptable toward solving several power systems-related issues is the adaptive neuro-fuzzy inference system (ANFIS) [50]. The adaptive neuro-fuzzy inference system (ANFIS) is an FL expert system that has been augmented with the learning abilities of ANN for supervised learning [51]. It has become one of the vital faces of contemporary data analytics and predictive systems [52]. ANFIS was used several times for predicting power systems parameters and determining the specific operating conditions of power systems. The ANFIS model based on association rules and trained by the Harris hawks optimization algorithm for monitoring effective VSM of a power system was developed in [53]. The capacity of the proposed hybrid ANFIS model for VSM assessment is explored in three essential parts: feature selection, model training, and data estimation. In [54], a fusion of support vector regression (SVR) and ANFIS models was developed for online voltage stability assessment based on synchronized phasor measurements. The SVR-ANFIS parameters are optimally tuned using the ant lion optimizer (ALO) to achieve adequate model training for precise performance.

In [55], the hybridization of the NN using the multi-layer perceptron (MLP) and ANFIS was proposed, developed, and compared for monitoring the power system's VSM based on the power system's information from phasor measurement units (PMUs). In the proposed hybrid MLP-MSA and ANFIS-MSA models, the moth swarm algorithm (MSA) algorithm is adopted to optimize the model parameters. The ANFIS model and its hybridized variants are famous for their ability to handle information based on linguistics using fuzzy rules, combined with the capabilities for processing numbers [56]. ANFIS is also known for its clarity in data exploitation with limited operator involvement and its ability to be trained faster with significantly lower computational memory requirements [57]. Thus, studies have been repleted with different real-life engineering applications of ANFIS, ranging from pollution management and environmental sustainability [58,59] and sport prediction [60] to petroleum industry analysis [61], transportation [62], the field of medicine [63], social demography [64], and so on. For power system-related predictive analysis, several ML techniques including ANFIS and its variants have been significantly deployed for the prediction of the closeness of power system networks to voltage collapse. However, as observed from the literature, the input parameters are mostly limited to a few power system parameters such as voltage magnitudes and their phases [41,53,54] etc. Thus, the ANFIS-based voltage stability monitoring prediction model implemented in this study considered six significant power systems analysis parameters and the voltage stability margin is measured using the critical boundary index per unit of the system's base power. Moreover, the potential of the standalone ANFIS model and its hybridization with particle swarm optimization (PSO) for effective prediction is compared as discussed below.

3. Mathematical Modeling

3.1. Voltage Stability Margin (VSM)

For a simple transmission network model shown in Figure 1, i and k indicate the transmission network's sending and receiving end, P and Q are the active power and

reactive power loading at the buses, whilst V and δ are the bus voltage magnitude and angle. The line reactance and resistance are r and x , respectively.

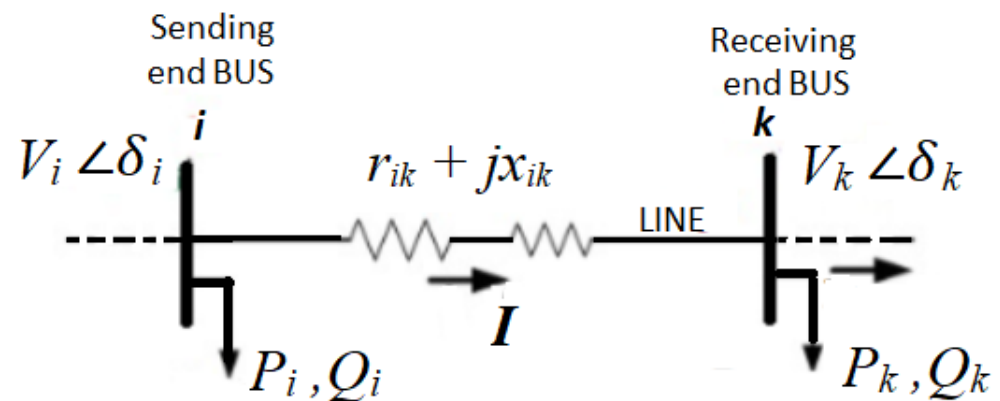


Figure 1. A two-node simplified transmission network [9].

Considering the line flow equations, the power transfer equation at the receiving end of the power system is obtained as given below:

$$P_k + jQ_k = (V_k \angle \delta_k) \left(\frac{V_i \angle \delta_i - V_k \angle \delta_k}{r_{ik} + jx_{ik}} \right)^* \quad (1)$$

The above Equation (1) is further resolved, as found in [4,65], to yield the simplified power transfer Equations (2) and (3) which wholly describes the voltage stability condition of power systems:

$$(P_k r_{ik} + x_{ik} Q_k) + j(P_k x_{ik} - r_{ik} Q_k) = V_i V_k \cos(\delta_i - \delta_k) - jV_i V_k \sin(\delta_i - \delta_k) - V_k^2 \quad (2)$$

$$V_k^4 + 2V_k^2 (P_k r_{ik} + Q_k x_{ik} - 0.5V_i^2) + (P_k^2 + Q_k^2) (r_{ik}^2 + x_{ik}^2) = 0 \quad (3)$$

For the given power system to be within a stable voltage stability operating limit, Equation (3) must have unique positive solutions (stable roots). Thus, the power system is voltage stability-proof when it fulfills the condition described by Equation (4):

$$\left(P_k r_{ik} + Q_k x_{ik} - 0.5V_i^2 \right)^2 + (P_k^2 + Q_k^2) (r_{ik}^2 + x_{ik}^2) \leq 0 \quad (4)$$

The critical boundary index (CBI) approach for VSM estimation was derived in [4] as an approach for directly approximating the real and reactive power loading distance of a power system network to the point of voltage collapse based on the criticality of the transmission lines. As shown in Figure 2, the stability boundary that describes the maximum real and reactive load that the power system can bear without the occurrence of voltage collapse (i.e., the VSM) is ruled by Equation (4). Consequently, CBI is calculated as the distance between the current operating point, $K(P_k, Q_k)$, and the critical point $C(X, Y)$ located on the stability boundary.

To obtain the solution to the critical operating point $C(X, Y)$, a constrained function (Equation (5)) is formed and solved using the Lagrange multiplier approach. The CBI values, obtained from Equation (6), give information about the VSM of the power system in per unit (pu) equivalent of the base MVA power. The susceptibility of the power network to voltage collapse due to transmission line failure is reflected by a low CBI value which indicates poor VSM.

$$F(X, Y, \lambda) = \left[(X - P_k)^2 + (Y - Q_k)^2 \right]^{\frac{1}{2}} - \lambda \left[(r_{ik} X + x_{ik} Y - 0.5V_i^2)^2 + (X^2 + Y^2) (r_{ik}^2 + x_{ik}^2) \right] \quad (5)$$

$$CBI = \left[(X - P_k)^2 + (Y - Q_k)^2 \right]^{\frac{1}{2}} \tag{6}$$

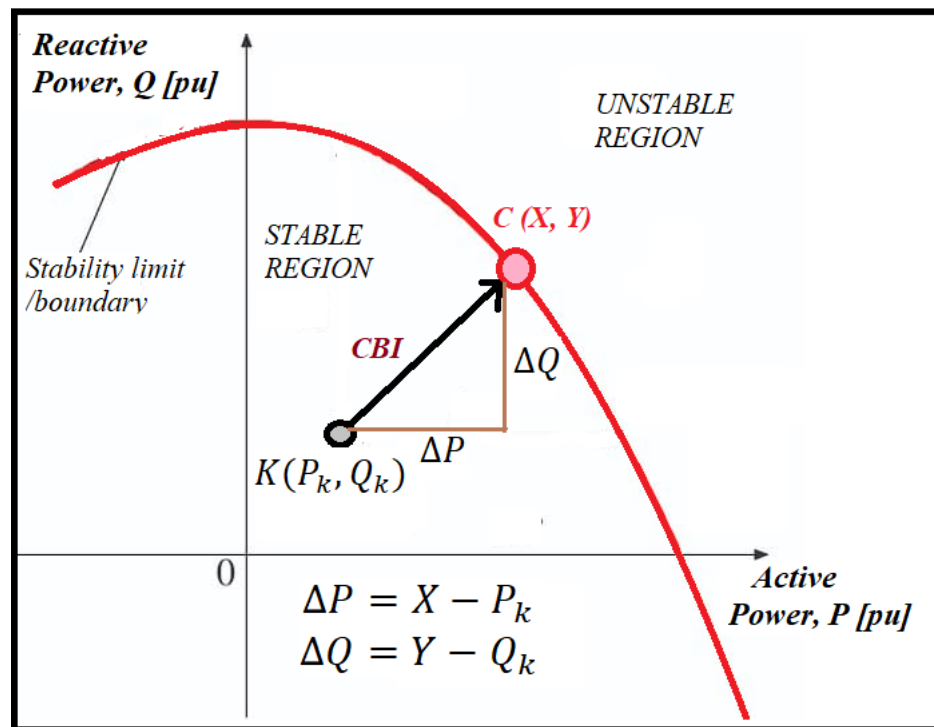


Figure 2. P–Q curve showing the voltage stability margin as a function to load increase [4].

3.2. ANFIS and PSO-ANFIS Implementation Procedures

The fundamental ANFIS model uses the ‘if–then’ probabilistic rules based on either Mamdani-type or Sugeno-type implementation qualitative decision-making purposes with no distinctive quantitative information [66]. The Takagi–Sugeno ANFIS model was implemented in this work using the hybrid rule of learning and backpropagation gradient descent with least square methods for pre-processing, and the optimal estimation of output parameters [67]. The five crucial parts of the ANFIS model are fuzzification, multiplication, normalization, de-fuzzification, and the summation final output by summation, as shown in Figure 3 [68]. The clustering technique used in implementing the ANFIS models discussed in this work is the fuzzy ‘c-Means’ clustering algorithm using fifteen (15) clusters [69].

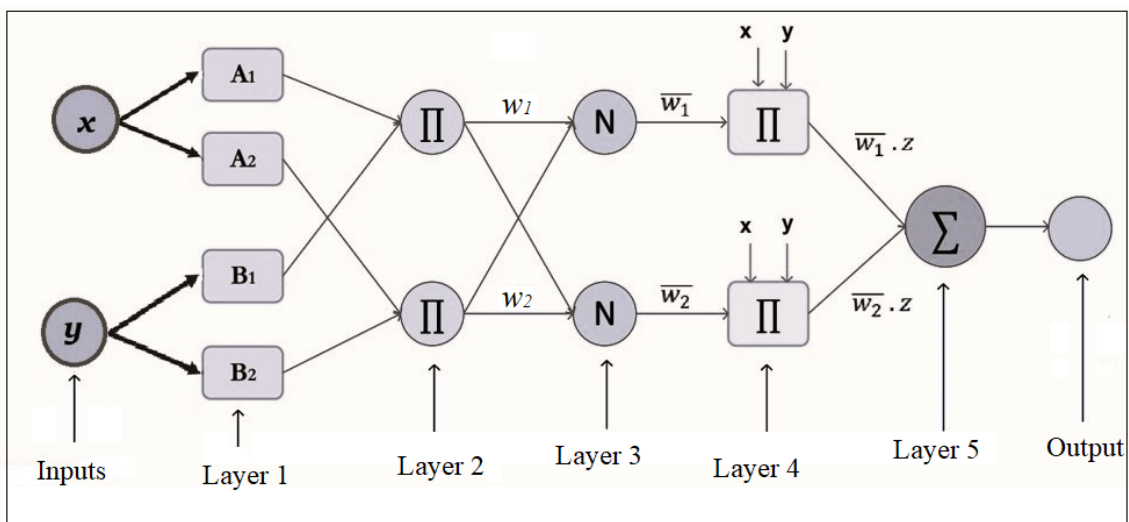


Figure 3. The five-layer architecture of the ANFIS model [69].

The implementation procedure for the ANFIS model is as described: for an ANFIS model with two inputs (x, y) and one output (f), two 'if-then' probabilistic rules are defined based on the first-order Takagi–Sugeno model given below:

Rule 1: if x is A_1 and y is B_1 , then:

$$f_1 = p_1 x + q_1 y + r_1$$

Rule 2: if x is A_2 and y is B_2 , then:

$$f_2 = p_2 x + q_2 y + r_2$$

where x and y are the inputs, A_k and B_k are the fuzzy sets, f_i are the outputs within a fuzzy rule, and p_k, q_k and r_k are the consequent parameters as obtained from the training process.

Layer 1: The fuzzification layer contains square adaptive nodes with fuzzy membership functions described by a set of inference rules as given below:

$$O_k^1 = \mu_{A_k}(x), \quad k = 1, 2 \quad (7)$$

$$O_k^1 = \mu_{B_k}(y), \quad k = 1, 2 \quad (8)$$

where O_k^1 is the membership grade of the fuzzy sets, which specifies the degree of agreement between the input (x, y). The fuzzy sets A_k and B_k, μ are the Gaussian membership functions that handle the degree of membership and quantify the grade of membership of the element within the fuzzy set.

Layer 2: At the next layer, i.e., the multiplication/product layer, the input values from the fuzzification layer are weighted based on the strength of each membership function and processed according to the pre-specified product rule. The node at this layer is fixed and non-adaptive; all the input values reaching this node are multiplied to determine the output at each node. The output is called the firing strength of a fuzzy rule and is estimated according to the equation below.

$$O_k^2 = w_k = \mu_{A_k}(x) \cdot \mu_{B_k}(y), \quad k = 1, 2 \quad (9)$$

Layer 3: This layer also consists of fixed and non-adaptive nodes. At this layer, all the calculated firing strengths are normalized by calculating the ratio of the firing strength of each rule to the total firing strength of all rules combined; i.e., the normalized firing strength of the k -th rule is obtained as shown below.

$$O_k^3 = \bar{w}_k = \frac{w_k}{w_1 + w_2}; \quad k = 1, 2 \quad (10)$$

Layer 4: This layer is the defuzzification layer, and it consists of adaptive nodes whose results are decoded from the set of inference rules used to code the input in layer 2. At this layer, a nodal first-order polynomial function is obtained by calculating the effect of the k -th rule on the output of the model; this is achieved by finding the product of the normalized firing strengths of the rule obtained from the third layer and expressed as a function of the consequent parameters as illustrated below:

$$O_k^4 = \bar{w}_k(p_k x + q_k y + r_k) = \bar{w}_k f_k, \quad k = 1, 2 \quad (11)$$

where \bar{w}_k is the normalized firing strengths of the rule, p_k, q_k and r_k are the consequent parameters, and f_i is a function of the output.

Layer 5: the last layer of the ANFIS architecture consists of a single non-adaptive node for summation. At this node, the final output is obtained by summing up all the incoming

values from layer 4. After that, all the results of the fuzzy classification processes are translated into appropriate concrete values.

$$O_k^5 = \sum_k \overline{w_k} f_k = \frac{\sum_k \overline{w_k} f_k}{\sum_k \overline{w_k}} \quad (12)$$

In this study, the performance of the ANFIS model implementation was enhanced by modifying the parameters and finetuning the prediction process using the particle swarm optimization (PSO) algorithm. PSO is an evolutionary optimization algorithm that was found to be effective for diverse optimization problems with various levels of intricacies [70]. PSO implementations involve two steps which are the estimation of the modification size/value, which is often called the velocity, and the update of the specific target function, which is referred to as ‘the position’; in this case, ‘the position’ will be the ANFIS parameters. The modification of the particle’s velocity is calculated as:

$$V_i^{k+1} = w \cdot V_i^k + c_1 \cdot r_1 \cdot (Pbest_i^k - X_i^k) + c_2 \cdot r_2 \cdot (Gbest^k - X_i^k) \quad (13)$$

The particle’s position is then updated using the calculated particle’s velocity as given:

$$X_i^{k+1} = X_i^k + V_i^{k+1} \quad (14)$$

where w is the weighting function, c_1 and c_2 , are the acceleration coefficients, r_1 and r_2 , are random numbers between 0 and 1, V_i^k and X_i^k are the current velocity and position of particle i at iteration k , V_i^{k+1} and X_i^{k+1} are the modified velocity and position of particle i , $P_{best_i}^k$ and $G_{best_i}^k$ are the personal and global bests of particle i . The dynamically changing inertia weight or weighting factor is employed because it guides the exploration and utilization of the search space, and it is expressed as [71].

$$w = w_{max} - \left(\frac{w_{max} - w_{min}}{max_{it}} \right) \times It \quad (15)$$

where w_{max} and w_{min} are the inertia weight’s final and initial values, respectively, It and max_{it} are current and maximum iteration numbers, respectively, whilst w_{max} and w_{min} are taken to be 0.4 and 0.9, respectively. The fitness function of the PSO-ANFIS parameters optimization procedure is the minimization of the root mean square error (RMSE) which is a measure of the deviation between the target values and the predicted outputs. The simplified illustration for the implementation of the PSO-ANFIS model is shown in Figure 4 and the PSO implementation parameters, as shown in Table 1, are selected considering their previous implementation in the literature [68].

Table 1. PSO parameters.

Parameter	Values
Population size	50
Number of iterations	200
Cognitive factor, C_1	2.0
Social factor, C_2	2.0
Inertia weight, w	0.9–0.4

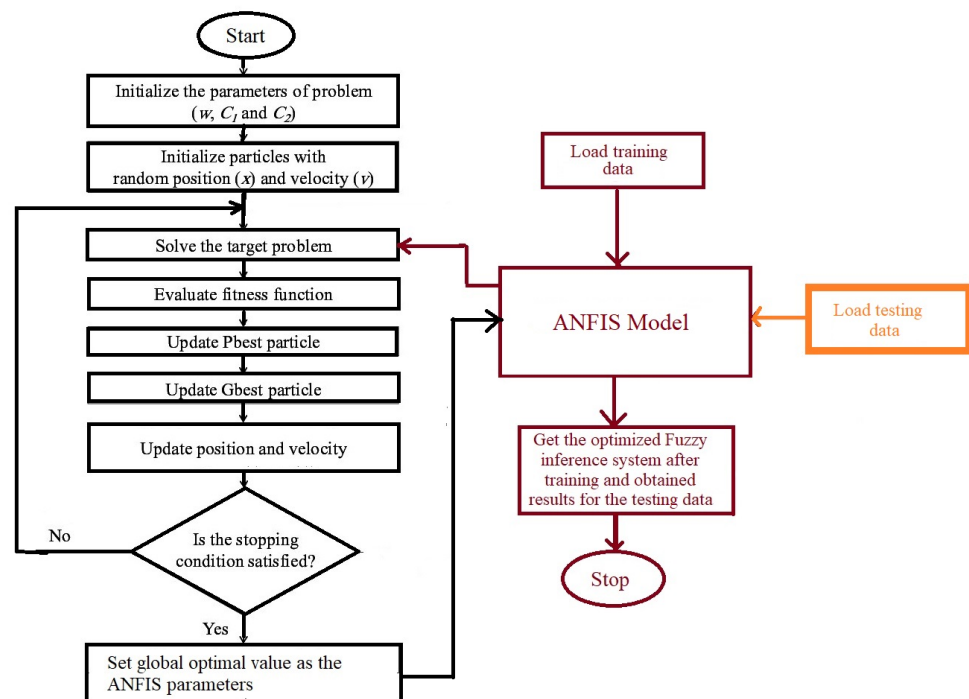


Figure 4. The simplified illustration for PSO-ANFIS training and testing.

3.3. FIS Model Performance Analysis

Based on the prediction errors, the performance of the developed ANFIS models is evaluated by the application of following performance-based statistical tools [69]:

- Root mean square error (RMSE):

$$RMSE = \sqrt{\frac{\sum_{n=1}^N [y_n - \hat{y}_n]^2}{N}} \quad (16)$$

- Mean absolute percentage error (MAPE):

$$MAPE = \frac{1}{N} \sum_{n=1}^N \left| \frac{y_n - \hat{y}_n}{y_n} \right| \times 100\% \quad (17)$$

- Coefficient of correlation (R):

$$R = \sqrt{1 - \left\{ \frac{\sum_{n=1}^N (y_n - \hat{y}_n)^2}{\sum_{i=1}^N (y_n - \bar{y})^2} \right\}} \quad (18)$$

where N is the data length, y_n , \hat{y}_n and \bar{y} are the calculated VSM values (targets), predicted VSM values (outputs) using the FIS models, and the mean of the calculated VSM values. The values of $RMSE$ and $MAPE$ show the model accuracy regarding the deviation of outputs from the true values (targets). Thus, the lower the values of $RMSE$ and $MAPE$, the better the performance of the FIS model. Pearson's correlation shows the agreement of the predicted data with the target using regression analysis, and R should have a value close to 1.0 to indicate the effectiveness of the prediction model.

3.4. PSO-ANFIS Optimization Procedure for CBI Prediction

The primary optimization problem for ANFIS parameter tuning using the PSO algorithm is described below. The considered fitness function is the minimization of the root mean square error (RMSE):

$$\text{minimize } RMSE = \sqrt{\frac{\sum_{n=1}^N [y_n - \hat{y}_n]^2}{N}} \quad (19)$$

The constraints are the load flow and critical boundary conditions as described below:

$$P_k - V_k \sum_{k \neq i, i=1}^{N_{bus}} V_i [G_{ik} \cos \delta_{ik} + B_{ik} \sin \delta_{ik}] = 0 \quad (20)$$

$$Q_k - V_k \sum_{k \neq i, i=1}^{N_{bus}} V_i [G_{ik} \sin \delta_{ik} - B_{ik} \cos \delta_{ik}] = 0 \quad (21)$$

$$V_k^{min} \leq V_k \leq V_k^{max} \quad \forall k; k \in N_{bus} \quad (22)$$

$$|S_{L_k}| \leq S_{L_k}^{max} \quad \forall k; k \in N_{br}. \quad (23)$$

$$CBI_k \geq CBI_k^{lim}. \quad \forall k; k \in N_{br}. \quad (24)$$

Equation (24) is the stability constraint and $S_{L_k}^{max}$ is the line flow limit. The stability limits on the power flow along a transmission line can be as low as 20% of the line's thermal limit [72,73]. Thus:

$$CBI_k^{lim} = 0.2 \times S_{L_k}^{max} \quad \forall k; k \in n_{tl} \quad (25)$$

where $N_{br.}$ is the total number of lines/branches and N_{bus} is the number of buses/nodes.

4. Simulation Procedure and Results' Discussion

The model development and simulation was performed using Matlab 2022a (student version) on a PC workstation with 64-bit data configuration and Intel(R) Core(TM), i7-8650U processor at an average speed of 1.90GHz (2112 Mhz, 4 core(s), 8 logical processor(s)).

4.1. Description of Case Studies and Data Pre-Processing for ANFIS Model Implementation

Six important operation parameters of power systems are considered as the input data; these are: line resistance r_{ik} , line reactance x_{ik} , active power injected at the receiving bus P_k , reactive power injected at the receiving bus Q_k , the sending end voltage magnitude V_i and the voltage angle δ_{ik} . The target output is the VSM using critical boundary index (CBI) values. The real and reactive powers increase in small steps and from the base loads and the Newton–Raphson (NR)-based load, flow analysis is run for the base loading and each load step while ensuring the tractability (convergence) of the NR power flow solution. The information obtained from the NR load flow analysis are the independent/input parameters $P_k, Q_k, V_i, \delta_{ik}$ and the dependent/output parameter CBI, while the line parameters r_{ik} and x_{ik} are directly obtained from the power system line data. Alongside the base load, five additional load levels are generated using a load incremental step of 10% of the base load, i.e., at a base load, and [base load + (10%, 20%, 30%, 40% and 50%)], respectively.

Thus, the total length L_{data} of the data for ANFIS implementation is $(6 \times N_{br.})$ and the size of the data is $(6 \times N_{br.})$ by 7, where $N_{br.}$ is the number of lines/branches in the network. For the development of the ANFIS-VSI model, 75% of the entire data length is selected the training data and the remaining 25% are considered the testing data. The two test cases considered in this work are the standard IEEE 30-bus system and the Nigerian 28-bus system and the details of both systems are contained in [73]. The IEEE 30-bus system has forty-one (41) transmission lines, $N_{br.}$; thus, the total data length, L_{data} , is 246, out of which 185 of the data length are used for training and the remaining 61 are used for testing the

ANFIS model. For the other test case, the Nigerian 28-bus system has fifty-two transmission lines, $N_{br.}$; thus, the total data length, L_{data} , is 312 and 234 of the total data length are used for training while the remaining 78 were deployed for testing the developed ANFIS model. The simple illustration of the considered ANFIS models and the input parameters and output information link is shown in Figure 5.

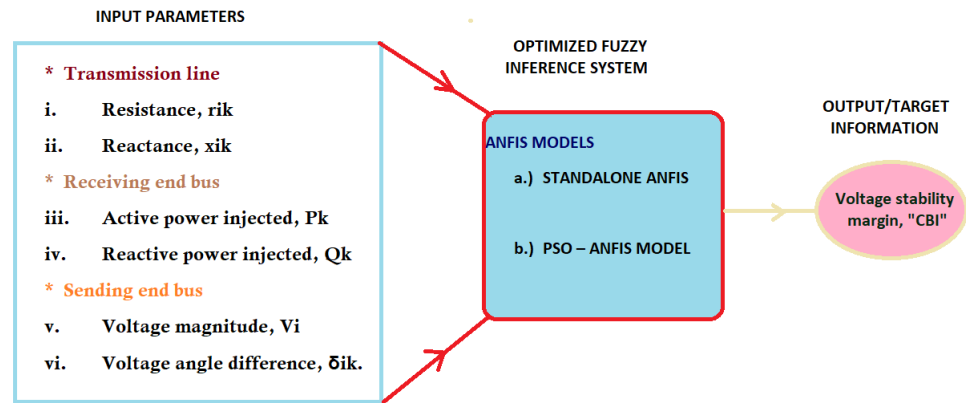


Figure 5. Illustration of the developed ANFIS model architecture.

4.2. Discussion of Results

The data plots showing the trend of the predicted CBI values using ANFIS and PSO-ANFIS against the target CBI values and the corresponding regression analysis are presented in Figures 6 and 7 for the standard IEEE 30-bus system, respectively. Moreover, plot of the predicted CBI values versus the target values and the regression analysis for the Nigerian 28-bus system are illustrated in Figures 8 and 9, respectively. Finally, the detailed analysis of the performance of the developed ANFIS models using the statistical error-based analysis and the regression tool for both systems are summarized in Table 2 for a concise comparison and detailed discussion of findings.

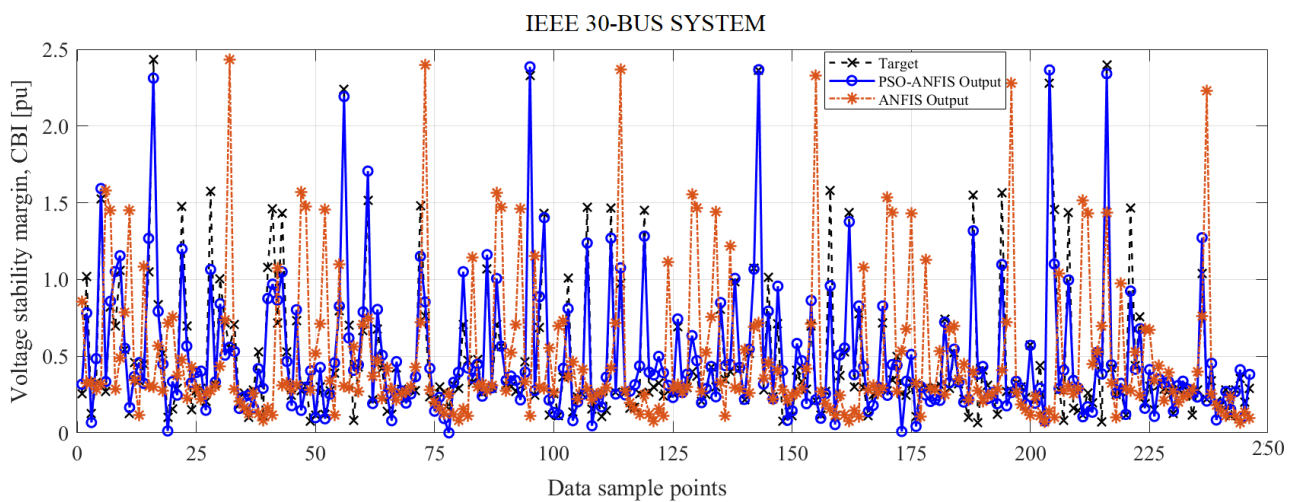


Figure 6. Plot of target (calculated) and output (predicted) VSM values for IEEE 30-bus system.

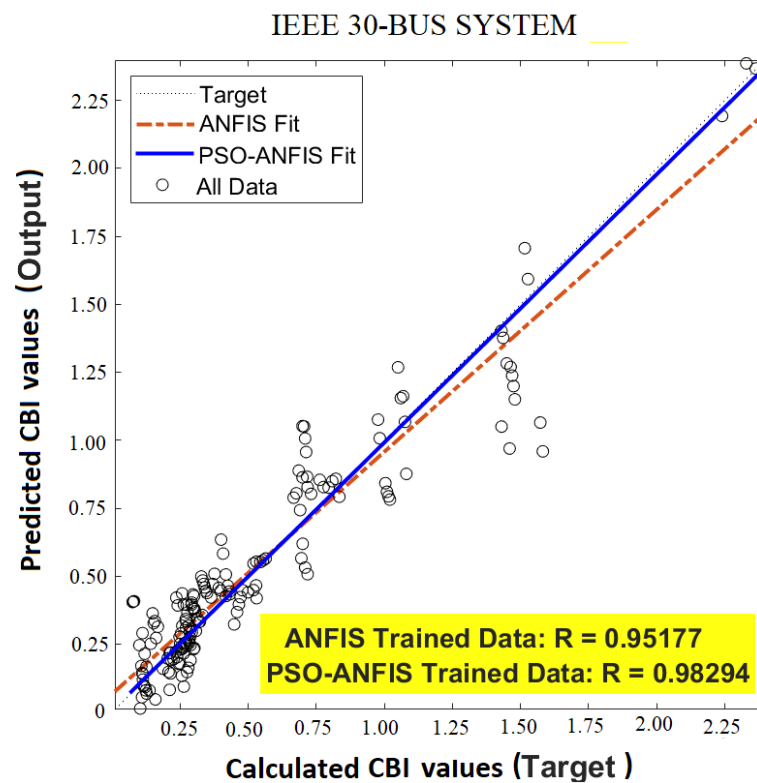


Figure 7. Regression plots for IEEE 30-bus system.

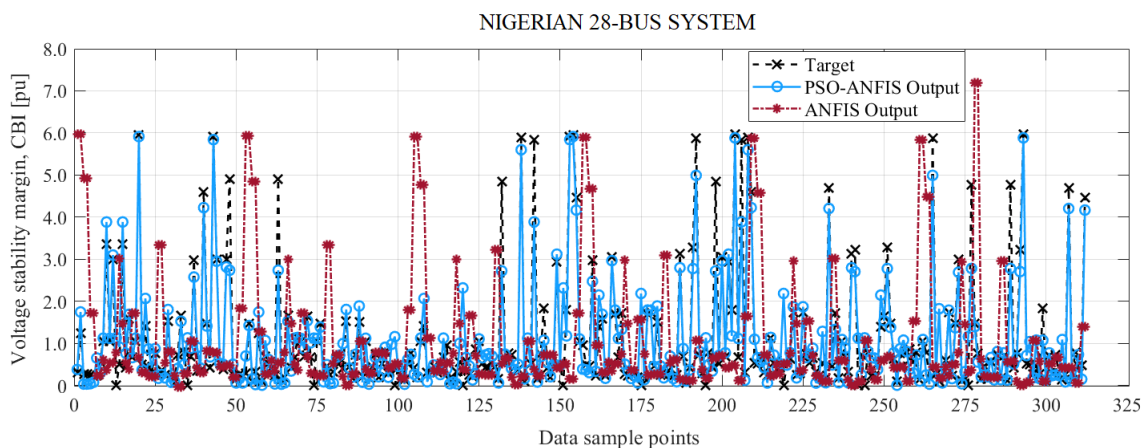


Figure 8. Plot of target (calculated) and output (predicted) VSM values for NIGERIAN 28-bus system.

Considering the standard IEEE 30-bus system with 41 transmission lines corresponding to 246 data points for six different load levels, with the values of $RMSE = 0.1795$ and $RMSE = 0.5833$ for PSO-ANFIS and ANFIS models, respectively, the developed models performed considerably. However, PSO-ANFIS performs better than the ANFIS prediction model in terms of deviation between the expected output and the predicted output as validated by the mean absolute percentage error at $MAPE = 5.5876\%$ for PSO-ANFIS against $MAPE = 13.6002\%$ for the standalone ANFIS model. The regression analysis using the R values shows that the correlation between the target and the predicted outcomes for both FIS models shows positive results, as indicated by values significantly close to the ideal value, which is $R = 1.0$. With $R = 0.9829$ and $R = 0.9518$, for PSO-ANFIS and ANFIS models, respectively; with the hybrid, PSO-ANFIS performs slightly better. However, the simulation time of 182.5 min for PSO-ANFIS (in 200 iterations) against 24.5 min for

standalone ANFIS, which indicates the need to prioritize either accuracy or time when deciding which of the models to deploy for real-time voltage stability condition monitoring.

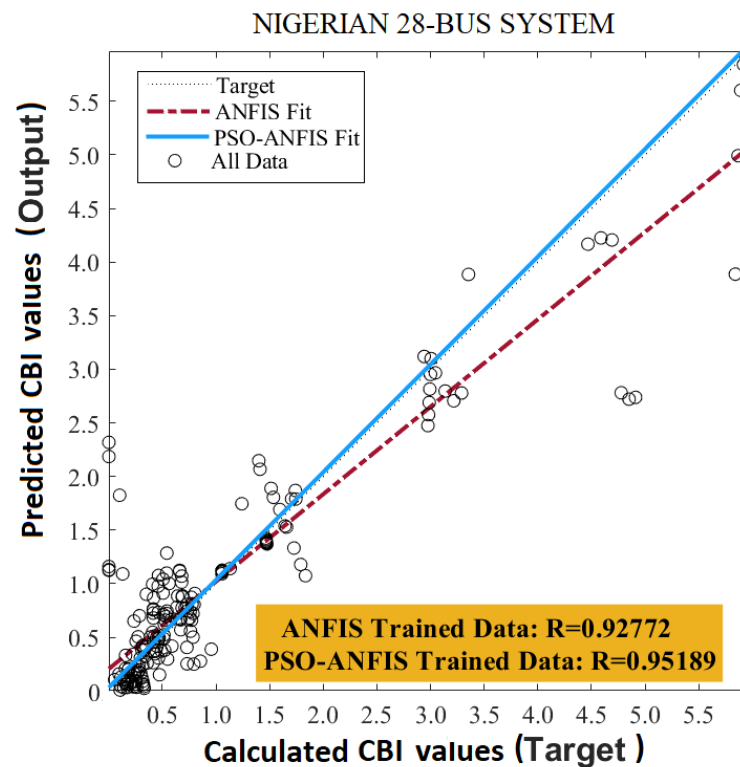


Figure 9. Regression plots for NIGERIAN 28-bus system.

The Nigerian 28-bus system has 52 transmission lines (branches), corresponding to 312 sampling points considering the six loading conditions. The performance of the developed ANFIS and PSO-ANFIS models for effectively predicting the power systems VSM is observed to be substantially accurate. The two statistical error analysis and the regression analysis allude to the effectiveness of both models, with the hybrid ANFIS model performing comparatively better. The lower estimated value of $RMSE = 2.3247$ and $MAPE = 8.1705\%$ for PSO-ANFIS as against $RMSE = 5.5024$ and $MAPE = 8.1705$ for ANFIS shows the superiority of the PSO-ANFIS. The regression analysis shows the R values for both ANFIS models to be within the extremely strong positive correlation range of $0.9 \leq R \leq 1.0$; and PSO-ANFIS shows better performance at $R = 0.9519$ against the ANFIS model with $R = 0.9277$. The time for PSO-ANFIS implementation is significantly higher than that of PSO due to the optimization process involved in achieving the FIS initial parameters. The computational time can increase with the number of iterations required to achieve the optimal performance of the PSO-ANFIS model.

Table 2. Model performance comparison for both test cases.

Test Systems	FIS Models	Performance Analysis			Comp. Time (mins)
		RMSE	MAPE (%)	R	
IEEE 30-BUS	ANFIS	0.5833	13.6002	0.9518	24.5
	PSO-ANFIS	0.1795	5.5876	0.9829	182.5
NIGERIAN 28-BUS	ANFIS	5.5024	19.9504	0.9277	57.2
	PSO-ANFIS	2.3247	8.1705	0.9519	212.7

5. Conclusions

Developing efficient techniques for predicting the voltage instability levels of power systems using artificial intelligence and machine learning is one of the exciting areas of power system research in recent times. Based on the existing works on voltage stability analysis in the steady-state, stability level of power systems mainly depends on some voltage and power injection parameters. Based on these parameters, this study developed and evaluated the performance of the standalone ANFIS model and PSO-ANFIS hybrid model for predicting the voltage stability margin of power systems using the critical boundary index (CBI) approach. Both models are tested on the standard IEEE 30-bus network and the Nigerian 28-bus system using six different load levels. Error-based performance metrics, such as *RMSE*, *MAPE*, and *R* are considered to compare the effectiveness of the ANFIS and PSO-ANFIS variants for VSM monitoring. Consequently, the performance of the PSO-ANFIS model is found to be superior in terms of the percentage reduction in prediction error and the results obtained from the regression analysis. Finally, the performance of the PSO-ANFIS model in terms of simulation time and memory consumption can be enhanced using supercomputer workstations and parallel computing techniques, which opens this work to further research.

Author Contributions: O.B.A.—conceptualization, resource, modeling and writing; K.A.F.—proofreading and supervision; D.T.O.O.—resource and proofreading; E.I.O.—resource and validation. All authors have read and agreed to the published version of this manuscript.

Funding: This research received no external funding.

Institutional Review Board Statement: Not applicable.

Informed Consent Statement: Not applicable.

Data Availability Statement: The main data used for this work are the bus and line parameters for the standard IEEE 30-bus and the Nigerian 28-bus networks [73].

Acknowledgments: Special thanks to M. Furukakoi for providing the Matlab files for voltage stability analysis and P. Adedeji for providing the Matlab files for the PSO-ANFIS model.

Conflicts of Interest: The authors declare no conflict of interest.

References

1. Adhikari, A.; Naetiladdanon, S.; Sagswang, A.; Guring, S. Comparison of Voltage Stability Assessment using Different Machine Learning Algorithms. In Proceedings of the 2020 IEEE 4th Conference on Energy Internet and Energy System Integration (EI2), Wuhan, China, 30 October–1 November 2020; pp. 2023–2026.
2. Cutsem, T.V.; Vournas, C. *Voltage Stability of Electric Power Systems*, 3rd ed.; Kluwer: Norwell, MA, USA, 2003.
3. Canizares, C.A.; De Souza, A.C.; Quintana, V.H. Comparison of performance indices for detection of proximity to voltage collapse. *IEEE Trans. Power Syst.* **1996**, *11*, 1441–1450. [[CrossRef](#)]
4. Furukakoi, M.; Adewuyi, O.B.; Danish, M.S.S.; Howlader, A.M.; Senjyu, T.; Funabashi, T. Critical Boundary Index (CBI) based on active and reactive power deviations. *Int. J. Electr. Power Energy Syst.* **2018**, *100*, 50–57. [[CrossRef](#)]
5. Dobson, I.; Lu, L. New methods for computing a closest saddle node bifurcation and worst case load power margin for voltage collapse. *IEEE Trans. Power Syst.* **1993**, *8*, 905–913. [[CrossRef](#)]
6. Taylor, C.W. *Power System Voltage Stability*, 1st ed.; McGraw-Hill: Palo Alto, CA, USA, 1994.
7. Danish, M.S.S.; Senjyu, T.; Danish, S.M.S.; Sabory, N.R.; Mandal, P. A recap of voltage stability indices in the past three decades. *Energies* **2019**, *12*, 1544. [[CrossRef](#)]
8. Kumar, R.; Mittal, A.; Sharma, N.; Duggal, I.V.; Kumar, A. PV and QV curve analysis using series and shunt compensation. In Proceedings of the 2020 IEEE 9th Power India International Conference (PIICON), Murthal, India, 28 February–1 March 2020; pp. 1–6.
9. Adewuyi, O.B.; Adeagbo, A.P.; Adebayo, I.G.; Howlader, H.O.R.; Sun, Y. Modified analytical approach for PV-DGs integration into a radial distribution network considering loss sensitivity and voltage stability. *Energies* **2021**, *14*, 7775. [[CrossRef](#)]
10. Laplante, P.; Milojicic, D.; Serebryakov, S.; Bennett, D. Artificial intelligence and critical systems: From hype to reality. *Computer* **2020**, *53*, 45–52. [[CrossRef](#)]
11. Sarker, I.H. Ai-based modeling: Techniques, applications and research issues towards automation, intelligent and smart systems. *SN Comput. Sci.* **2022**, *3*, 1–20. [[CrossRef](#)]

12. Monti, A.; Ponci, F. Electric power systems. In *Intelligent Monitoring, Control, and Security of Critical Infrastructure Systems*, 1st ed.; Kyriakides, E., Polycarpou, M., Eds.; Springer: Berlin/Heidelberg, Germany, 2015.
13. Laughton, M. Artificial intelligence techniques in power systems. In Proceedings of the IEE Colloquium on Artificial Intelligence Techniques in Power Systems (Digest No: 1997/354), London, UK, 3 November 1997; p. 1.
14. Ongsakul, W.; Dieu, V.N. *Artificial Intelligence in Power System Optimization*; CRC Press: Boca Raton, FL, USA, 2013.
15. Yousuf, H.; Zainal, A.Y.; Alshurideh, M.; Salloum, S.A. Artificial intelligence models in power system analysis. In *Artificial Intelligence for Sustainable Development: Theory, Practice and Future Applications*; Springer: Berlin/Heidelberg, Germany, 2021; pp. 231–242.
16. El-Keib, A.; Ma, X. Application of artificial neural networks in voltage stability assessment. *IEEE Trans. Power Syst.* **1995**, *10*, 1890–1896. [[CrossRef](#)]
17. Rahi, O.; Yadav, A.K.; Malik, H.; Azeem, A.; Kr, B. Power system voltage stability assessment through artificial neural network. *Procedia Eng.* **2012**, *30*, 53–60. [[CrossRef](#)]
18. Singh, P.; Parida, S.; Chauhan, B.; Choudhary, N. Online Voltage Stability Assessment Using Artificial Neural Network considering Voltage stability indices. In Proceedings of the 2020 21st National Power Systems Conference (NPSC), Gandhinagar, India, 17–19 December 2020; pp. 1–5.
19. La Scala, M.; Trovato, M.; Torelli, F. A neural network-based method for voltage security monitoring. *IEEE Trans. Power Syst.* **1996**, *11*, 1332–1341. [[CrossRef](#)]
20. Nakawiro, W.; Erlich, I. Online voltage stability monitoring using artificial neural network. In Proceedings of the 2008 Third International Conference on Electric Utility Deregulation and Restructuring and Power Technologies, Nanjing, China, 6–9 April 2008; pp. 941–947.
21. Popović, D.; Kukolj, D.; Kulić, F. Monitoring and assessment of voltage stability margins using artificial neural networks with a reduced input set. *IEE Proc.-Gener. Transm. Distrib.* **1998**, *145*, 355–362. [[CrossRef](#)]
22. Goh, H.; Chua, Q.; Lee, S.; Kok, B.; Goh, K.; Teo, K. Evaluation for voltage stability indices in power system using artificial neural network. *Procedia Eng.* **2015**, *118*, 1127–1136. [[CrossRef](#)]
23. Jayasankar, V.; Kamaraj, N.; Vanaja, N. Estimation of voltage stability index for power system employing artificial neural network technique and TCSC placement. *Neurocomputing* **2010**, *73*, 3005–3011. [[CrossRef](#)]
24. Ashraf, S.M.; Gupta, A.; Choudhary, D.K.; Chakrabarti, S. Voltage stability monitoring of power systems using reduced network and artificial neural network. *Int. J. Electr. Power Energy Syst.* **2017**, *87*, 43–51. [[CrossRef](#)]
25. Bahmanyar, A.; Karami, A. Power system voltage stability monitoring using artificial neural networks with a reduced set of inputs. *Int. J. Electr. Power Energy Syst.* **2014**, *58*, 246–256. [[CrossRef](#)]
26. Li, S.; Ajarapu, V. Real-time monitoring of long-term voltage stability via convolutional neural network. In Proceedings of the 2017 IEEE Power & Energy Society General Meeting, Chicago, IL, USA, 16–20 July 2017; pp. 1–5.
27. Ibrahim, A.M.; El-Amary, N.H. Particle Swarm Optimization trained recurrent neural network for voltage instability prediction. *J. Electr. Syst. Inf. Technol.* **2018**, *5*, 216–228. [[CrossRef](#)]
28. Rao, A.N.; Vijayapriya, P. A robust neural network model for monitoring online voltage stability. *Int. J. Comput. Appl.* **2019**, 1–10. [[CrossRef](#)]
29. Fu, Y.; Chung, T. A hybrid artificial neural network (ANN) and Ward equivalent approach for on-line power system voltage security assessment. *Electr. Power Syst. Res.* **2000**, *53*, 165–171. [[CrossRef](#)]
30. Handschin, E.; Kuhlmann, D.; Rehtanz, C. Visualization and analysis of voltage stability using self-organizing neural networks. In Proceedings of the International Conference on Artificial Neural Networks, Lausanne, Switzerland, 8–10 October 1997; pp. 1113–1118.
31. Modi, P.; Singh, S.P.; Sharma, J. Loadability margin calculation of power system with SVC using artificial neural network. *Eng. Appl. Artif. Intell.* **2005**, *18*, 695–703. [[CrossRef](#)]
32. Chakraborty, K.; De, A.; Chakrabarti, A. Voltage stability assessment in power network using self organizing feature map and radial basis function. *Comput. Electr. Eng.* **2012**, *38*, 819–826. [[CrossRef](#)]
33. Duraipandy, P.; Devaraj, D. Extreme learning machine approach for on-line voltage stability assessment. In Proceedings of the International Conference on Swarm, Evolutionary, and Memetic Computing, Chennai, India, 19–21 December 2013; pp. 397–405.
34. Suganyadevi, M.; Babulal, C. Online voltage stability assessment of power system by comparing voltage stability indices and extreme learning machine. In Proceedings of the International Conference on Swarm, Evolutionary, and Memetic Computing, Chennai, India, 19–21 December 2013; pp. 710–724.
35. Villa-Acevedo, W.M.; López-Lezama, J.M.; Colomé, D.G. Voltage stability margin index estimation using a hybrid kernel extreme learning machine approach. *Energies* **2020**, *13*, 857. [[CrossRef](#)]
36. Hagmar, H.; Tong, L.; Eriksson, R.; Le Anh, T. Voltage instability prediction using a deep recurrent neural network. *IEEE Trans. Power Syst.* **2020**, *36*, 17–27. [[CrossRef](#)]
37. Sajjan, K.; Kumar, V.; Tyagi, B. Genetic algorithm based support vector machine for on-line voltage stability monitoring. *Int. J. Electr. Power Energy Syst.* **2015**, *73*, 200–208. [[CrossRef](#)]
38. Poursaeed, A.H.; Namdari, F. Real-time voltage stability monitoring using weighted least square support vector machine considering overcurrent protection. *Int. J. Electr. Power Energy Syst.* **2022**, *136*, 107690. [[CrossRef](#)]

39. Duraipandy, P.; Devaraj, D. On-line voltage stability assessment using least squares support vector machine with reduced input features. In Proceedings of the 2014 International Conference on Control, Instrumentation, Communication and Computational Technologies (ICCICCT), Kanyakumari, India, 10–11 July 2014; pp. 1070–1074.
40. Naganathan, G.; Babulal, C. Optimization of support vector machine parameters for voltage stability margin assessment in the deregulated power system. *Soft Comput.* **2019**, *23*, 10495–10507. [[CrossRef](#)]
41. Amroune, M.; Bouktir, T.; Musirin, I. Power system voltage stability assessment using a hybrid approach combining dragonfly optimization algorithm and support vector regression. *Arab. J. Sci. Eng.* **2018**, *43*, 3023–3036. [[CrossRef](#)]
42. Dharmapala, K.D.; Rajapakse, A.; Narendra, K.; Zhang, Y. Machine learning based real-time monitoring of long-term voltage stability using voltage stability indices. *IEEE Access* **2020**, *8*, 222544–222555. [[CrossRef](#)]
43. Liu, S.; Shi, R.; Huang, Y.; Li, X.; Li, Z.; Wang, L.; Mao, D.; Liu, L.; Liao, S.; Zhang, M.; et al. A data-driven and data-based framework for online voltage stability assessment using partial mutual information and iterated random forest. *Energies* **2021**, *14*, 715. [[CrossRef](#)]
44. Pinzón, J.D.; Colomé, D.G. Real-time multi-state classification of short-term voltage stability based on multivariate time series machine learning. *Int. J. Electr. Power Energy Syst.* **2019**, *108*, 402–414. [[CrossRef](#)]
45. Su, H.Y.; Lin, Y.J.; Chu, C.C. Applications of Decision Tree and Random Forest Methods for Real-Time Voltage Stability Assessment Using Wide Area Measurements. In *Wide Area Power Systems Stability, Protection, and Security*; Springer: Berlin/Heidelberg, Germany, 2021; pp. 373–391.
46. Wu, T.; Zhang, Y.J.A.; Wen, H. Voltage stability monitoring based on disagreement-based deep learning in a time-varying environment. *IEEE Trans. Power Syst.* **2020**, *36*, 28–38. [[CrossRef](#)]
47. Li, Y.; Zhang, M.; Chen, C. A deep-learning intelligent system incorporating data augmentation for short-term voltage stability assessment of power systems. *Appl. Energy* **2022**, *308*, 118347. [[CrossRef](#)]
48. Zhang, M.; Li, J.; Li, Y.; Xu, R. Deep learning for short-term voltage stability assessment of power systems. *IEEE Access* **2021**, *9*, 29711–29718. [[CrossRef](#)]
49. Ashfaq, M. A Tribute to Father of Fuzzy Set Theory and Fuzzy Logic (Dr. Lotfi A. Zadeh). *Int. J. Swarm Intell. Evol. Comput.* **2018**, *7*, 2.
50. Modi, P.; Singh, S.P.; Sharma, J. Fuzzy neural network based voltage stability evaluation of power systems with SVC. *Appl. Soft Comput.* **2008**, *8*, 657–665. [[CrossRef](#)]
51. Mendel, J.M. Type-2 fuzzy sets as well as computing with words. *IEEE Comput. Intell. Mag.* **2019**, *14*, 82–95. [[CrossRef](#)]
52. Jang, J.S. ANFIS: Adaptive-network-based fuzzy inference system. *IEEE Trans. Syst. Man Cybern.* **1993**, *23*, 665–685. [[CrossRef](#)]
53. Ghaghishpour, A.; Koochaki, A. An intelligent method for online voltage stability margin assessment using optimized ANFIS and associated rules technique. *ISA Trans.* **2020**, *102*, 91–104. [[CrossRef](#)]
54. Amroune, M.; Musirin, I.; Bouktir, T.; Othman, M.M. The amalgamation of SVR and ANFIS models with synchronized phasor measurements for on-line voltage stability assessment. *Energies* **2017**, *10*, 1693. [[CrossRef](#)]
55. Amroune, M.; Bourzami, A.; Zellagui, M.; Musirin, I. Real-time voltage stability monitoring using machine learning-based pmu measurements. In *Wide Area Power Systems Stability, Protection, and Security*; Springer: Berlin/Heidelberg, Germany, 2021; pp. 423–448.
56. Walia, N.; Singh, H.; Sharma, A. ANFIS: Adaptive neuro-fuzzy inference system—A survey. *Int. J. Comput. Appl.* **2015**, *123*, 32–38. [[CrossRef](#)]
57. Srisaeng, P.; Baxter, G.S.; Wild, G. An adaptive neuro-fuzzy inference system for forecasting Australia’s domestic low cost carrier passenger demand. *Aviation* **2015**, *19*, 150–163. [[CrossRef](#)]
58. Prasad, K.; Gorai, A.K.; Goyal, P. Development of ANFIS models for air quality forecasting and input optimization for reducing the computational cost and time. *Atmos. Environ.* **2016**, *128*, 246–262. [[CrossRef](#)]
59. Adeleke, O.; Akinlabi, S.A.; Jen, T.C.; Dunmade, I. Prediction of municipal solid waste generation: An investigation of the effect of clustering techniques and parameters on ANFIS model performance. *Environ. Technol.* **2022**, *43*, 1634–1647. [[CrossRef](#)] [[PubMed](#)]
60. Şahin, M.; Erol, R. A comparative study of neural networks and ANFIS for forecasting attendance rate of soccer games. *Math. Comput. Appl.* **2017**, *22*, 43. [[CrossRef](#)]
61. Panapakidis, I.P.; Dagoumas, A.S. Day-ahead natural gas demand forecasting based on the combination of wavelet transform and ANFIS/genetic algorithm/neural network model. *Energy* **2017**, *118*, 231–245. [[CrossRef](#)]
62. Atmaca, H.; Cetisli, B.; Yavuz, H.S. The comparison of fuzzy inference systems and neural network approaches with ANFIS method for fuel consumption data. In Proceedings of the Second International Conference on Electrical and Electronics Engineering Papers ELECO, Bursa, Turkey, 7–11 November 2001; Volume 6, pp. 1–4.
63. Nagy, E.; Puskás, M.; Drexler, D.A. Comparison of artificial neural network and ANFIS for parameter estimation of a tumor model. In Proceedings of the 2022 IEEE 20th Jubilee World Symposium on Applied Machine Intelligence and Informatics (SAMII), Poprad, Slovakia, 19–22 January 2022; pp. 000133–000140.
64. Ghobadiha, Y.; Motieyan, H. Urban growth modelling in Qazvin, Iran: An investigation into the performance of three ANFIS methods. *J. Spat. Sci.* **2022**, 1–20. [[CrossRef](#)]
65. Juanuwattanukul, P.; Masoum, M.A.S.; Niyomsak, C.; Mohseni, M. Voltage analysis for placement of DG in multiphase distribution networks. In Proceedings of the 2012 IEEE Power and Energy Society General Meeting, San Diego, CA, USA, 22–26 July 2012; pp. 1–5. [[CrossRef](#)]

66. Adedeji, P.A.; Akinlabi, S.A.; Madushele, N.; Olatunji, O.O. Hybrid neurofuzzy investigation of short-term variability of wind resource in site suitability analysis: A case study in South Africa. *Neural Comput. Appl.* **2021**, *33*, 13049–13074. [[CrossRef](#)]
67. Singh, R.; Kainthola, A.; Singh, T. Estimation of elastic constant of rocks using an ANFIS approach. *Appl. Soft Comput.* **2012**, *12*, 40–45. [[CrossRef](#)]
68. Adedeji, P.A.; Akinlabi, S.; Madushele, N.; Olatunji, O.O. Wind turbine power output very short-term forecast: A comparative study of data clustering techniques in a PSO-ANFIS model. *J. Clean. Prod.* **2020**, *254*, 120135. [[CrossRef](#)]
69. Adedeji, P.A.; Akinlabi, S.; Madushele, N.; Olatunji, O.O. Hybrid adaptive neuro-fuzzy inference system (ANFIS) for a multi-campus university energy consumption forecast. *Int. J. Ambient Energy* **2022**, *43*, 1685–1694. [[CrossRef](#)]
70. Valle, Y.D.; Venayagamoorthy, G.K.; Mohagheghi, S.; Hernandez, J.C.; Harley, R.G. Particle swarm optimization: Basic concepts, variants and applications in power systems. *IEEE Trans. Evol. Comput.* **2008**, *12*, 171–195. [[CrossRef](#)]
71. Rathore, A.; Sharma, H. Review on inertia weight strategies for particle swarm optimization. In *Proceedings of the Sixth International Conference on Soft Computing for Problem Solving*; Springer: Berlin/Heidelberg, Germany, 2017; pp. 76–86.
72. What Limits Power Flow Through an Overhead Transmission Line? 2013. Available online: www.pdc-cables.com/oh_limits_powerflow.pdf (accessed on 15 August 2022).
73. Adewuyi, O.B.; Howlader, H.O.R.; Olaniyi, I.O.; Konneh, D.A.; Senjyu, T. Comparative analysis of a new VSC-optimal power flow formulation for power system security planning. *Int. Trans. Electr. Energy Syst.* **2020**, *30*, e12250. [[CrossRef](#)]